ORGANOMETALLICS

Article

pubs.acs.org/Organometallics

Monomeric Rhodium(II) Complexes Supported by a Diarylamido/Bis(phosphine) PNP Pincer Ligand and Their Reactivity Toward Dihydrogen

Dan A. Smith,[†] David E. Herbert,[†] Justin R. Walensky,[‡] and Oleg V. Ozerov*[,†]

[†]Department of Chemistry, Texas A&M University, 3255 TAMU, College Station, Texas 77842, United States

[‡]Department of Chemistry, University of Missouri, Columbia, Missouri 65211, United States

Supporting Information

ABSTRACT: A rhodium(II) complex of a diarylamido/bis(phosphine) PNP pincer ligand, (PNP)Rh(OTf) (**2**, where OTf = O_3SCF_3 and PNP = [κ^3-*P*,*N*,*P*-(4-Me-2-($^iPr_2P$)-C_6H_3)$_2$N]), has been prepared by oxidation of the rhodium(I) precursor (PNP)Rh($H_2C{=}CHBu^t$) (**1**) with AgOTf. A series of related rhodium(II) complexes of the general formula (PNP)Rh(X) (where X = OAc (**3**), $OSiPh_3$ (**4**), OC_6H_4F (**5**), Cl (**6**)) was synthesized via simple anion metathesis reactions starting from **2**. In addition, complexes **3** and **6** could be prepared by hydrogen atom abstraction from (PNP)Rh(H)(OAc) (**7**) or (PNP)Rh(H)(Cl) (**8**) with TEMPO ((2,2,6,6-tetramethylpiperidin-1-yl)oxyl). Solid-state X-ray structures of compounds **2**−**6** revealed an approximately square-planar environment about Rh. Analysis of the structural features of **2**−**6**, EPR spectroscopic data, and DFT computational studies are most consistent with a +2 oxidation state for rhodium. Reactions of **2**, **3**, **5**, and **6** with H_2 were explored. The reaction of **2** with H_2 gave the new complex (PN(H)P)Rh(H)$_2$(OTf) (**9**), and the reaction of **3** with H_2 produced (PNP)Rh(H)(OAc) (**7**), whereas the reaction of **5** with H_2 gave the known (PNP)Rh(H_2) (**10**), all with complete consumption of the starting rhodium(II) complexes. In contrast, the reaction of **6** with H_2 produced a mixture of (PNP)Rh(H)(Cl) (**8**) and (PN(H)P)Rh(H)$_2$(Cl) (**11**) in apparent equilibrium with **6** and H_2. (PNP)Rh(H_2) (**10**) was identified as an elongated dihydrogen complex.

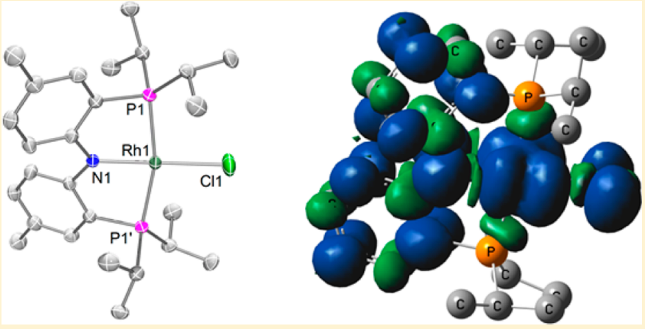

INTRODUCTION

In recent years there has been a growing interest in the chemistry of metalloradical complexes,[1] with their potential to homolytically cleave challenging bonds making them candidates for a wide range of processes, including CC activation,[2−4] olefin oxidation,[5] and hydrogen atom transfer.[6] For rhodium, isolated monomeric open-shell species of the +2 oxidation state are uncommon relative to +1 and +3 oxidation states, in part due to the well-established Rh^I/Rh^{III} oxidative addition chemistry.[7,8] Rh^{II} complexes are most often encountered as bimetallic species with a metal−metal bond supported by a set of bridging ligands, with chiral dirhodium tetracarboxylates notably successful for asymmetric metal carbenoid mediated catalysis.[9] Monomeric Rh^{II} complexes without chelating ligands are very rare, with their synthesis and isolation hindered by disproportionation reactions.[7,8,10−12] Instead, access to monomeric Rh^{II} often depends on a sterically cumbersome environment at the metal center to disfavor dimerization. To date, the exploration of Rh^{II} species has primarily focused on porphyrin-ligated complexes that have been shown to be capable of supporting a variety of X−H activations at Rh(II) (where X = Si, C, H, O).[13−16] Wayland et al. demonstrated that methane and the alkyl C−H bonds of toluene can be split under mild conditions at a (TMP)Rh^{II} porphyrin complex (where TMP = tetramesitylporphyrinato dianion), which exists in equilibrium with its dimeric form [(TMP)Rh]$_2$.[17,18] Furthermore, using tetratolylporphyrin (TTP) as a scaffold for rhodium(II), Chan et al. reported ring opening of cyclooctane, giving rise to a (TPP)Rh(*n*-octyl) complex in high yields.[2] The application of the *fac*-coordinating ligand *N*,*N*-bis(2-pyridylmethyl)amine (DPA) to rhodium and iridium by de Bruin et al. has led to the exploration of the reactivity of (DPA)M^{II}(COD) and other related metalloradicals.[19,20]

Pincer ligands[21] are particularly well-suited for supporting square-planar complexes, a geometry expected for low-spin Rh^{II}. Few examples of pincer supported Rh^{II} complexes, however, are known. The groups of Tilley and Bergman have demonstrated that bis(oxazoline) pincer ligated Rh^{II} complexes are capable of olefin cyclopropanation with ethyl diazoacetate,[22,23] and Milstein and co-workers have reported sterically congested Rh(II) complexes of the 2,6-bis((di-*tert*-butylphosphino)methyl)pyridine ligand.[24]

Received: August 7, 2012

dx.doi.org/10.1021/om300760j | *Organometallics* XXXX, XXX, XXX−XXX

Scheme 1. Syntheses of Complexes 2−8

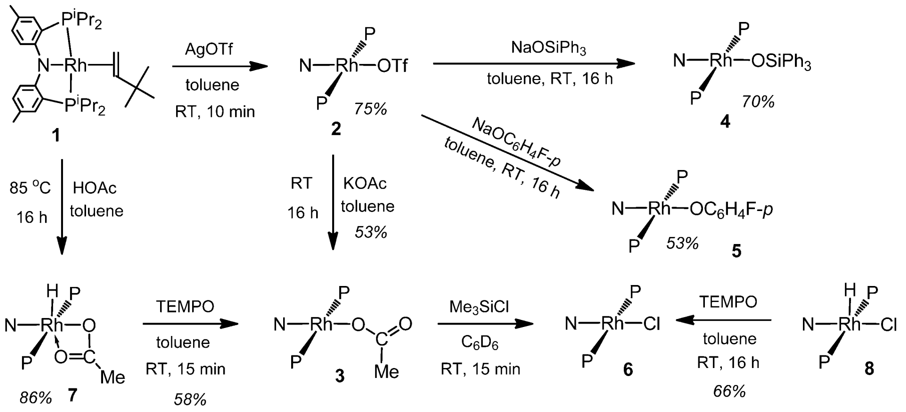

The diarylamido-based PNP ligand class[25−27] has proven to be a very useful supporting ligand for metals across the periodic table, in various oxidation states, including a number of species with unusual structure or reactivity.[28−36] We have previously reported on the chemistry of PNP complexes of Rh in the context of Rh^I/Rh^{III} reactivity.[37−46] It was envisaged that both the steric bulk and conformational rigidity of this PNP pincer would also allow for well-defined, square-planar Rh^{II} species. The synthesis of one of these compounds has been previously communicated.[43] PNP complexes of cobalt, the lighter congener of rhodium, in oxidation state +2 have been reported by Mindiola et al.[47] Herein, an exploration of a series of (PNP)Rh^{II}(X) complexes is presented, alongside computational studies to further the understanding of the nature of these species. Additionally, we report on the reactivity of (PNP)Rh^{II}(X) complexes with dihydrogen.

RESULTS AND DISCUSSION

Synthesis and Characterization. Addition of the one-electron oxidant AgOTf to the previously reported[41,45] Rh(I) precursor (PNP)Rh(H$_2$C=CH^{t}Bu) (**1**) in toluene successfully led to the corresponding rhodium(II) triflate complex (PNP)-Rh(OTf) (**2**), which was isolated in 75% yield (Scheme 1). The reaction was observed to be near-instantaneous, with a color change from orange to dark green and concomitant deposition of metallic silver clearly visible. ^{1}H NMR spectroscopic analysis of complex **2** revealed a set of broadened peaks, suggesting a paramagnetic species. Not all the expected proton resonances could be accounted for, presumably due to the extent of paramagnetic broadening. Analysis of the ^{19}F NMR spectrum of **2** revealed a resonance at −73.4 ppm, with this value likely influenced by the paramagnetic environment. No resonances were observed by ^{31}P NMR spectroscopy.

Attempts to extend this synthetic pathway to the use of AgOAc for the synthesis of the corresponding (PNP)Rh^{II} acetate complex led to a mixture of species. Instead, the synthesis of (PNP)Rh(OAc) (**3**), (PNP)Rh(OSiPh$_3$) (**4**), and (PNP)Rh(OC$_6$H$_5$F) (**5**) was possible by salt metathesis of **2** in toluene with KOAc, NaOSiPh$_3$, and NaOC$_6$H$_5$F, respectively (Scheme 1). Reaction of **3** with Me$_3$SiCl in C$_6$D$_6$ rapidly gave (PNP)RhCl (**6**), as detected by ^{1}H NMR spectroscopy, with Me$_3$SiOAc as the byproduct.

Another facile route to complexes **3** and **6** was envisaged via hydrogen atom abstraction from the corresponding Rh^{III} hydride complexes, similarly to the precedent in the work of Chan et al.[48] The bond dissociation energy (BDE) of a typical Rh^{III}−H bond falls within the 55−60 kcal/mol range,[18,49,50] and therefore, TEMPO did appear to be an appropriate hydrogen atom abstractor (the BDE for TEMPO-H is 69.6 kcal/mol).[51] (PNP)Rh(H)(κ^2-OAc) (**7**) was synthesized in high yield by the addition of an excess of acetic acid to **1**. For complex **7**, the hydride resonance of −23.77 ppm in the ^{1}H NMR spectra is downfield of the −29.91 ppm value for (PNP)Rh(H)(Cl) (**8**),[37] in accordance with the now filled coordination site trans to the hydride. The ^{31}P NMR spectroscopic resonances are similar for complexes **7** (52.7 ppm (J_{RhP} = 107 Hz)) and **8** (50.6 ppm (J_{RhP} = 105 Hz)), though the chromophores of each are notably different, with the former exhibiting a red coloration and the latter an intense green. Upon addition of an equimolar amount of TEMPO to **7** or **8**, consumption of the rhodium hydride complex was noted in the ^{1}H NMR spectra with concurrent generation of broad resonances identifiable as the desired Rh(II) species. The conversion of **7** to **3** is accompanied by a distinctive color change from red to dark green. The greater solubility of TEMPO-H in nonpolar solvents allowed the isolation of the organometallic complexes in reasonable yields by recrystallization. This synthesis of **6** from **8** has been previously communicated.[43]

The isolation of **2−6** as green, semicrystalline materials allowed for their characterization with combustion analysis, confirming the proposed formulations of the bulk samples. Measurements of the magnetic moment in solution by the Evans method gave values in the range 1.9−2.1 μ_{B}, representative of complexes with a single unpaired electron and in accordance with reported monomeric Rh(II) compounds.[11,24] In recent years, many ligands have been found to display noninnocent behavior toward metal centers under certain circumstances.[52] The PNP pincer is no exception, with Mindiola et al. demonstrating that the oxidation of [(PNP)-Ni(Cl)] to [(PNP)Ni(Cl)][OTf] occurs at the ligand with the metal remaining in the +2 oxidation state.[53] To this end it was of interest to interrogate a (PNP)Rh^{II}X compound by electron paramagnetic resonance (EPR) spectroscopy. Collection of the EPR spectrum of complex **2** at ambient temperature in toluene (Figure 1) gave a broad unresolved signal with a *g* value of 2.19, corresponding well to other reported Rh(II) *g* values.[54,55] At lower temperatures the signal was not found to sharpen and remains broad.

X-ray Structural Studies. Fortunately, single crystals suitable for a set of X-ray diffraction studies could be grown for compounds **2−6**, allowing their structural elucidation (Figure 2 and Table 1). Complexes **2−6** were found to be

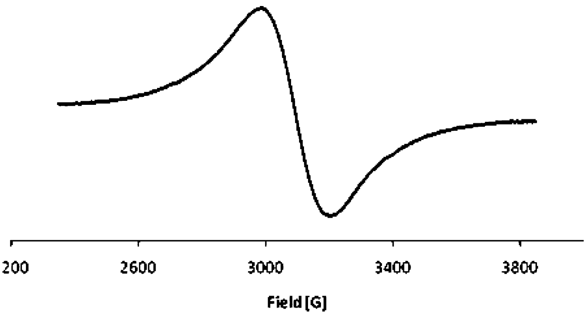

Figure 1. X-band EPR spectrum of complex **2** obtained at 293 K in toluene.

monomeric, with the PNP ligand binding in a meridional fashion to give an approximately square planar geometry at the four-coordinate rhodium center, as expected for low-spin Rh^{II}.[8] The geometries of the corresponding (PNP)Rh fragments in these five compounds were found to be very similar to each other. The slightly shorter Rh−N distance in **2** in comparison to those in **3**−**6** can be read as the manifestation of the weaker trans-influence character of the triflate trans to N. Likewise, the spread of Rh−O distances in **2**−**5** appears to reflect the relative basicity of the oxygenous ligands: the shortest Rh−O distance was recorded for the strongest O-donor (triphenylsiloxide in **4**), and the longest Rh−O distance was recorded for the weakest O-donor (triflate in **2**).

The most notable structural feature of the series is the contraction of the Rh−N bond relative to the PNP compounds of Rh^{I} and Rh^{III} that have been previously characterized. In the Rh^{I} compounds (PNP)Rh($H_2C{=}CH^tBu$) (**1**) and (PNP)Rh(−N≡N−)Rh(PNP),[41] the Rh−N_{PNP} distances were found to be 2.062(4) and 2.0358(12)/2.0444(12) Å, respectively. Interestingly, the Rh−N_{PNP} distances in five-coordinate, approximately square pyramidal Rh^{III} complexes fall into the same 2.02−2.06 Å range, as well: (PNP)Rh(Me)(Cl), 2.059(4) Å;[37] (PNP)Rh(Ph)(Br), 2.048(5) Å;[39] (PNP)Rh(Me_2SiCl)(Cl), 2.027(2) Å.[42] The octahedral Rh^{III} complex (PNP)Rh(Ph)(κ^2-O_2CNEt_2)[46] possesses a similar Rh−N bond distance of 2.044(2) Å. On the other hand, the Rh−N distances in the five Rh^{II} complexes (**2**−**6**) reported here all fall within a narrow 1.93−1.97 Å range (Table 1).

Moreover, the X-ray molecular structure of (PNP)RhCl (**6**) allows a direct comparison with the analogous palladium complex (PNP)PdCl previously reported.[26] A shortening of the metal−nitrogen distance is noted upon moving from palladium (2.0258(19) Å) to rhodium (1.968(2) Å), in contrast to the expected contraction of bond length for a transition metal of a later group. A similar contrast is evident in comparing the metal−nitrogen distance in (PNP)Rh(OAc) (**3**; 1.968(3) Å) with that of the closely analogous (^{F}PNP)Pd(OAc) (2.015(5) Å).[56]

The lone pair of the amido group of PNP is potentially capable of a π-interaction with a metal orbital. In square-planar Rh^{I} or Pd^{II} (d^8) complexes, and in square-pyramidal or octahedral Rh^{III} (d^6) complexes, the matching d orbitals of the metal are doubly filled, leading to a four-electron two-center p_π−d_π repulsion or, at least, a lack of π-bonding. However, in a square-planar Rh^{II} complex (d^7), a half-filled d_π orbital provides for a three-electron, two-center π-interaction, which may be thought of as a half-order π-bond.

Inspection of the C−N bonds of the ligand scaffold of **2** reveals a slight elongation (1.418(2) Å) relative to those of Rh(I) (e.g.: (PNP)Rh($H_2C{=}CH^tBu$), 1.394(6) and 1.403(5) Å; (PNP)Rh(N_2)Rh(PNP), 1.3952(18), 1.3899(18), 1.3930(18), and 1.3953(18) Å).[41] The other Rh^{II} complexes

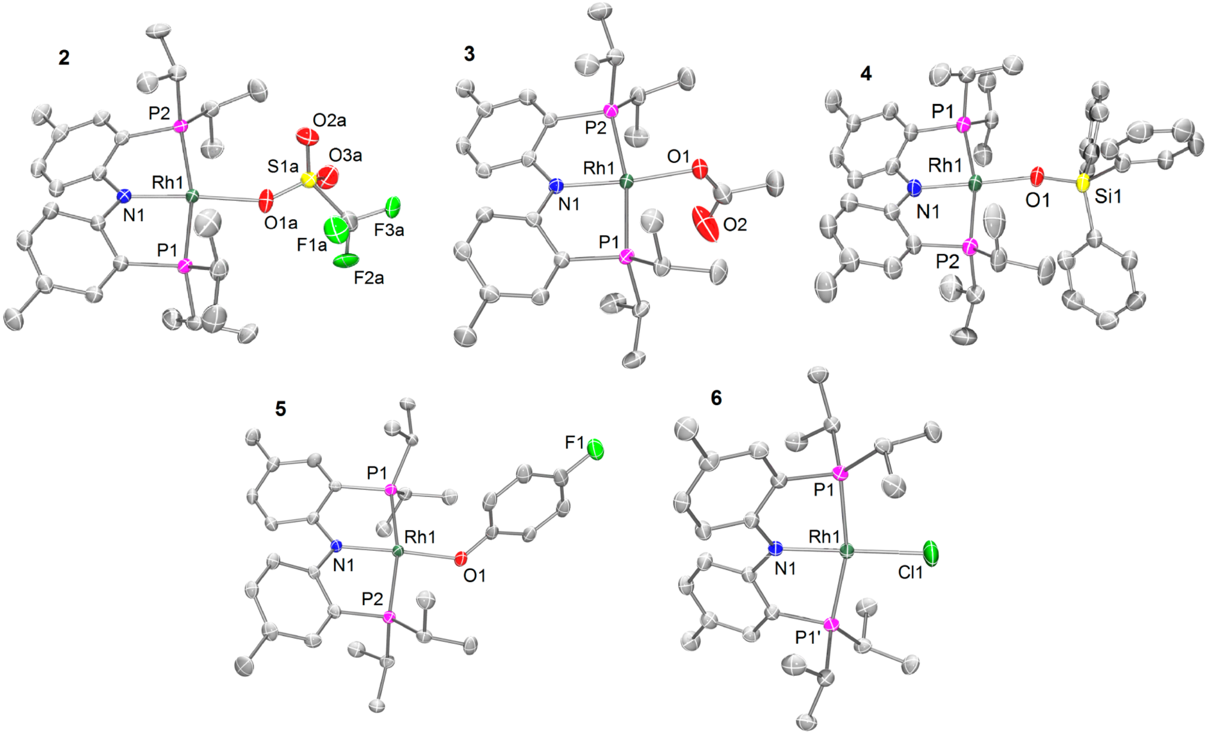

Figure 2. POV-Ray rendition[57] of the ORTEPs[58] of complexes **2**−**6** (ellipsoids set to 50% probability) showing selected atom labeling. The following were omitted for clarity: (a) hydrogen atoms in all structures; (b) one of the two disordered triflate positions in **2**.

Table 1. Selected Bond Distances (Å) and Angles (deg) in the Solid State Structures of Complexes 2–6

	2	3	4	5	6
Rh1–P1	2.3085(7)	2.2941(13)	2.298(8)	2.2962(14)	2.2905(9)
Rh1–P2	2.3228(6)	2.2834(14)	2.309(9)	2.2920(13)	2.2905(9)
Rh1–N1	1.9324(14)	1.968(3)	1.961(6)	1.959(2)	1.968(2)
Rh1–X	2.1073(13)	2.065(3)	2.002(5)	2.023(2)	2.3230(13)
P1–Rh1–P2	165.778(16)	168.55(3)	166.52(7)	166.73(3)	164.60(3)
N1–Rh1–X	175.39(6)	171.43(11)	177.33(13)	177.31(10)	180
X	O(Tf)	O(Ac)	$O(SiPh_3)$	$O(C_6H_4F\text{-}p)$	Cl

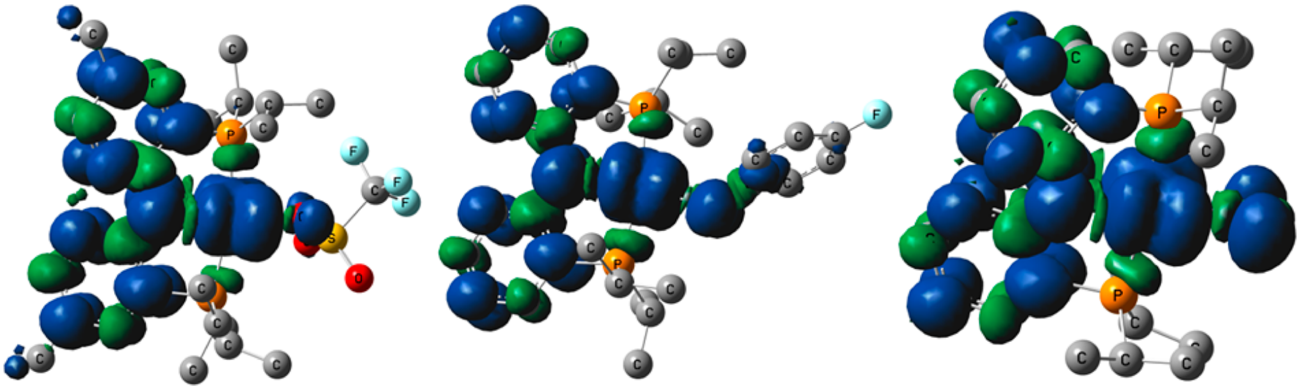

Figure 3. Spin density plots of **2** (left), **5** (center), and **6** (right).

3–**6** show similarly elongated C–N distances, while the C–N distances in the aforementioned structures of Rh^{III} and Pd^{II} complexes are shorter, at ca. 1.39–1.40 Å (where resolution of the determination and lack of disorder allow such comparisons). Thus, the elongation of the C–N bonds in the Rh^{II} complexes is slight but very consistent. It can be interpreted as indicative of the greater π-donation from N to Rh resulting in a lesser π-interaction between the aryl rings and the amide lone pair.

Computational Studies. To further explore the electronic structure, a computational study was undertaken with complexes **2**, **5**, and **6**. Optimization (Rh and P, B3LYP/Stuttgart; H, C, N, F, and O, B3LYP/6-31G(d′)) gave bond lengths and angles in good agreement with those of the X-ray molecular structure. The calculated spin density plots are shown in Figure 3. The spin densities at Rh were calculated to be 0.65, 0.70, and 0.72 in **2**, **5**, and **6**, respectively. This supports the Rh(II) formulation, although with a significant contribution from the ligand, and fits the conclusion of a two-center, three-electron Rh–N π-bond we arrived at on the basis of the crystallographic metrics. The lack of resolved hyperfine coupling in the EPR spectrum of **2** can be attributed to the significant delocalization of the free electron over the PNP ligand.

Reactions with H_2. Vlugt and co-workers have recently reported the activation of H_2 by a tripodal tetraphosphine-supported Rh^{II} complex.[59] The complex $[(PP_3)Rh(Cl)][PF_6]$ (where PP_3 = tris(N-diphenylphosphino-3-methylindolyl)phosphine) was found to undergo reaction with molecular hydrogen at 5 bar over a period of 12 h. The authors proposed a mechanism involving an outer sphere redox process to Rh(I) followed by protonation to give the resultant $[(PP_3)Rh(Cl)(H)][PF_6]$.

It was of interest therefore to explore the potential of complexes **2**–**6** for splitting molecular hydrogen (Scheme 2). Exposure of a solution of complex **3** to an atmosphere of hydrogen gas gave rise to a color change from dark green to light red with the consumption of starting material apparent by NMR spectroscopy in 15 min, with concurrent formation of **7**. This corresponds to net addition of a hydrogen atom to **3**, and the favorability of this reaction makes sense on the basis of BDE arguments. If the Rh–H BDE in **7** is indeed on the order of 55–60 kcal/mol,[18,49,50] formation of two such bonds should be enough to compensate for the cleavage of the H–H bond (104 kcal/mol), particularly since it is additionally favored by coordination of the second acetate oxygen.

Scheme 2

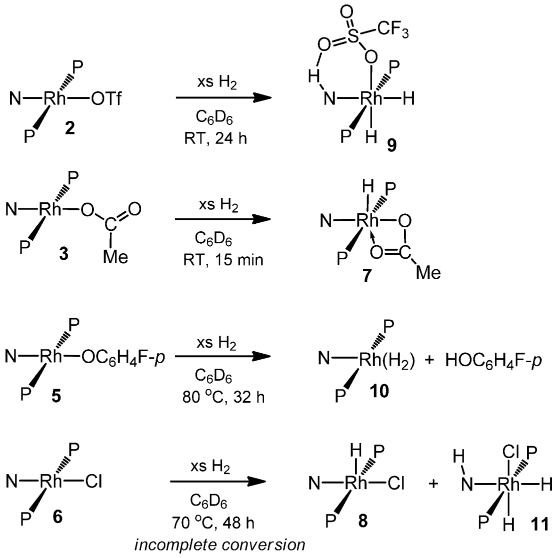

The reaction of **5** with H_2 yielded $(PNP)Rh(H_2)$ (**10**), which can be viewed as the consequence of hydrogenolysis of the putative intermediate (PNP)Rh(H)(OAr), by analogy with the formation of **7**. It is not surprising that the Rh–OAr bond is favorably hydrogenolyzed but the Rh–OAc bond is not. The latter should be a stronger Rh−O bond, and the binding of the acetate is additionally strengthened by the κ^2 coordination.

Yet another outcome was observed for **2**, where complete reaction, even with a large excess of molecular hydrogen at 1 atm, only occurred over a period of 24 h to yield a light yellow solution. Analysis of the solution by ^{1}H NMR spectroscopy revealed the single species **9**, possessing a multiplet resonance at −19.76 ppm and a singlet resonance at 9.51 ppm with an integration ratio of 2:1, the latter signal indicative of protonation at the amide functionality of the PNP pincer.[60] The signal at −19.76 ppm possesses a T_1 value of 541 ms at 25 °C and evolves into two signals (each of 1H intensity) at −16.2 and −23.2 ppm upon cooling to −63 °C. This is most consistent with the ground-state dihydride structure (PN(H)P)Rh(H)$_2$(OTf) with a kinetically facile degenerate exchange mechanism of the two hydride positions. In the related Pd(II) complex [(PN(H)P)PdH]$^+$, we previously determined that hydrogen bonding with the triflate anion shifts the resonance of an NH proton to around 9 ppm, as opposed to chemical shifts of around 7 ppm observed with weakly interacting anions, such as $[B(C_6H_3(CF_3)_2)_4]^-$ and $[HCB_{11}H_{11}]^-$.[61] It seems reasonable to expect the triflate in **9** to be hydrogen bonded to the NH proton. At the same time, the low-temperature ^{1}H NMR chemical shifts of the hydride signals of **9** are most consistent with one hydride (−16.2 ppm) trans to the NH and the other (−23.2 ppm) trans to a weak but present donor (such as triflate). A hydride trans to an empty site in a Rh^{III} square-pyramidal complex is expected to resonate at around −30 ppm.[37] These observations can be reconciled by the ground-state structure, in which the triflate is bound to Rh and hydrogen bonded to the NH proton, as depicted in Scheme 2. This assignment is consistent with the apparent C_s symmetry observed in the ^{1}H NMR spectra of **9**, where four environments are clearly evident for the methyl groups of the isopropyl moieties. Compound **9** can be regarded as arising from the putative intermediate (PNP)Rh(H)(OTf) via addition of H$_2$ across the metal−amido bond. The greater unsaturation of (PNP)Rh(H)(OTf) in comparison to **7** is the likely cause of the favorability of the heterolytic addition of H$_2$. The exchange process may well involve intermediate dissociation of triflate (or at least cleavage of the O−Rh bond) and conversion to a Rh^I dihydrogen complex. Analogous cationic Rh^I dihydrogen complexes with pyridine/bis(phosphine) PN*P pincer ligands have been reported.[62] Neutral (PCP)Rh(H$_2$) complexes have also been characterized as having dihydrogen ligands.[63]

Faced with the preponderance of pincer-supported Rh^I dihydrogen complexes, we also decided to examine the nature of (PNP)Rh(H$_2$) (**10**). Treatment of **2** with excess CaH$_2$ and D$_2$O generated (PNP)Rh(HD) (**10-*d***) in situ, for which a J_{HD} value of 18.3 Hz was measured. Low-temperature NMR experiments yielded a minimal value of 39 ms for T_1 relaxation, measured at −48 °C. On the basis of relationships between H−H distances and $T_{1,min}$ values or $J_{H\text{-}D}$ coupling established in the literature,[64] these data indicate a "stretched" or "elongated" dihydrogen complex,[65] with a predicted H−H distance of 1.13 Å.

Reacting **6** with H$_2$ (ca. 1 atm) produced a mixture of compounds we have identified as **8** and (PN(H)P)Rh(H)$_2$Cl (**11**), with some unreacted **6** and H$_2$ remaining. Addition of extra H$_2$ and heating did not result in complete conversion to **11**. The structure of **11** was tentatively established on the basis of the solution NMR data. Two distinct hydride environments of equal intensity at −16.68 and −18.33 ppm were observed, although both are broadened with no well-defined coupling. Additionally, a broad proton resonance was observed at 8.31 ppm, tentatively assigned to the NH proton. These data are consistent with an octahedral environment about the rhodium center, now in the oxidation state +3, with two hydrides in a cis arrangement; one trans to NH, another trans to Cl. We cannot reliably establish whether chloride is located syn or anti with respect to the N−H bond, but precedent exists for the *syn*-H−N−M−Cl orientation resulting in a weak H···Cl hydrogen-bonding interaction in a closely related pincer system.[66] Compound **11** exhibits a doublet resonance at 67.2 ppm with a J_{RhP} coupling constant of 114 Hz in its ^{31}P{^{1}H} NMR spectrum, comparable to those of **9** (65.1 ppm, d, 114 Hz). The hydride chemical shifts in **11** compare well to those of the reported complexes Rh(H)$_2$(Cl)(PPh$_3$)(Py)$_2$, (−17.2 and −18.0 ppm) and Rh(H)$_2$(Cl)(PPh$_3$)$_2$(Py) (−16.8 and −17.8 ppm), which possess hydrides trans to Cl and a nitrogen donor, analogously to **11**.[67,68] Compound **11** can be viewed as the product of heterolytic addition of H$_2$ across the N−Rh bond in **8**, whereas **8** can be viewed as analogous to **7** in being formed by net hydrogen atom addition to **6**. As chloride is more donating than a triflate, addition of H$_2$ to **8** to give **11** would be expected to be less favorable than addition of H$_2$ to **2** to give **9**.

This reactivity toward molecular hydrogen for complexes **2**−**6** is in stark contrast to the observed stability of rhodium(II) pincer complexes reported by Milstein and co-workers.[24] This is likely a consequence of the amido lone pair in our series that can participate in the heterolytic splitting, whereas in the examples presented by Milstein et al., the nitrogen atom of the pincer exists within a metal-bound pyridine ring and without an active lone pair of electrons.

■ CONCLUSION

Rhodium(II) complexes of the PNP pincer have been prepared and demonstrated to be stable and monomeric. These compounds are readily accessible in good yields by oxidation, hydrogen atom abstraction, or salt metathesis. Exploration of the nature of a few of the studied complexes by DFT calculations reveal that the spin density is manifested most greatly at Rh, but with significant delocalization into the ligand. (PNP)Rh^{II}X compounds readily reacted with H$_2$, and the nature of the products of these reactions depended heavily on the identity of X.

■ EXPERIMENTAL SECTION

General Considerations. Unless specified otherwise, all manipulations were performed under an argon atmosphere using standard Schlenk line or glovebox techniques. Toluene, diethyl ether, C$_6$D$_6$, THF, and pentane were dried over and distilled from NaK/Ph$_2$CO/18-crown-6 and stored over molecular sieves in an Ar-filled glovebox. Fluorobenzene and CDCl$_3$ were dried with and then distilled from CaH$_2$ and stored over molecular sieves in an Ar-filled glovebox. The following compounds were prepared according to literature procedures: (PNP)Rh(H$_2$C=CH^{t}Bu) (**1**)[45] and (PNP)Rh(H)(Cl) (**8**).[37] NaOSiPh$_3$ and KOC$_6$H$_4$F were synthesized by reaction of the corresponding silanol and alcohol with NaHMDS (HMDS = hexamethyldisilazide) and KO^{t}Bu, respectively. All other chemicals were purchased from either Aldrich or Acros and used as received unless otherwise noted. NMR spectra were recorded on a Varian Inova 300, Varian Mercury 300, or Varian NMRS 500 spectrometer. For ^{1}H and ^{13}C{^{1}H} NMR spectra, the residual solvent peak was used as an internal reference. ^{31}P NMR spectra were referenced externally using 85% H$_3$PO$_4$ at 0 ppm. ^{19}F NMR spectra were referenced externally using neat trifluoroacetic acid at −78.5 ppm. Chemical shifts are reported in ppm and coupling constants in Hz. The conventional inversion−recovery method was used to determine the variable-temperature longitudinal relaxation time T_1 (16−20 variable delays were used with the waiting time 5 times longer than the expected relaxation time). NMR spectroscopic measurements for both (PNP)-RhH_2 and (PN(H)P)Rh(H)$_2$(OTf) (**9**) were conducted on a Bruker AV 500 MHz NMR spectrometer. EPR spectra were recorded on an X-band Bruker EMS spectrometer with an Oxford ESR900 liquid He cryostat.

Computational Details. All B3LYP[69] (Becke-3 exchange[70] and Lee−Yang−Parr correlation[71] functional) calculations were performed using the Gaussian 09 suite of software.[72] Full geometry optimizations were performed, and stationary points were characterized via analytical frequency calculations using the Pople double-ζ quality basis set (6-31G(d′))[73,74] for the C, H, and N atoms, which contains a polarization (d) function on the C, N, and O atoms. The Stuttgart/Dresden (SDD) triple-ζ quality basis set (SDD) with an effective core potential (ECP)[75] for the Rh and P atoms was employed with an additional d basis function of 0.387 added for P.

Synthesis of (PNP)Rh(OTf) (2). To a solution of (PNP)Rh-($H_2C{=}CH^tBu$) (**1**; 1000 mg, 1.62 mmol) in toluene (8 mL) was added AgOTf (422 mg, 1.64 mmol), and a color change from orange to dark green was observed immediately. Removal of the volatile components in vacuo gave a residue which could be recrystallized as a green solid from pentane (824 mg, 75%). Single crystals suitable for an X-ray diffraction study were grown by cooling a saturated pentane solution. ^1H NMR (300 MHz, C_6D_6): δ 11.10 (2H, $\nu_{1/2}$ = 900), 3.92 (∼20H, $\nu_{1/2}$ = 470). ^{19}F NMR (282 MHz, C_6D_6): δ −73.4 (s). Anal. Calcd: C, 47.62; H, 5.92. Found: C, 47.72; H, 6.12. μ_{eff} (Evans NMR method) = 2.1 μ_B.

Synthesis of (PNP)Rh(OAc) (3). *Method 1.* To a solution of **2** (50 mg, 0.073 mmol) in toluene (5 mL) was added KOAc (8 mg, 0.08 mmol), and the mixture was stirred. After 16 h the volatile components were removed in vacuo, pentane was added, and the resultant solution was filtered through Celite. Concentration and cooling (−30 °C) gave rise to a green crystalline material that was isolated by filtration and washed with cold pentane (3 × 1 mL) (22 mg, 53%).

Method 2. To a solution of (PNP)Rh(H)(OAc) (**7**; 200 mg, 0.35 mmol) in toluene (10 mL) was added TEMPO (55 mg, 0.35 mmol), and a color change from red to dark green was observed within 15 min. Removal of the volatile components in vacuo gave a green residue which could be recrystallized as a green crystalline solid from pentane (116 mg, 58%). Single crystals suitable for an X-ray diffraction study were grown by cooling a saturated pentane solution. ^1H NMR (300 MHz, C_6D_6): δ 40.08 (2H, br), 37.43 (2H, br), 10.16−14.72 (6H, m, br), 5.43 (24H, br). MS (ESI$^+$): *m/z* 590 (M$^+$). Anal. Calcd: C, 56.95; H, 7.34. Found: C, 56.93; H, 7.39. μ_{eff} (Evans NMR method) = 2.0 μ_B.

Attempted Synthesis of (PNP)Rh(OAc) (3). To a solution of **1** (30 mg, 0.049 mmol) in toluene (8 mL) was added AgOAc (8 mg, 0.049 mmol), and a color change from orange to brown was observed over 15 min. Removal of the volatile components in vacuo and dissolution in C_6D_6 of the residue allowed the observation by NMR spectroscopy of predominantly starting material **1**, **3**, and a complex exhibiting a resonance by ^{31}P NMR spectroscopy at 66.8 (d, *J* = 134 Hz).

Synthesis of (PNP)Rh(OSiPh$_3$) (4). To a Young NMR tube containing a solution of **2** (60 mg, 0.088 mmol) in toluene (10 mL) was added $NaOSiPh_3$ (25 mg, 0.089 mmol), and the mixture was sonicated for 16 h. Removal of the volatile components in vacuo gave a green residue. Addition of CH_2Cl_2 (8 mL) and filtration through Celite gave a green solution. Concentrating (∼2 mL), layering with pentane, and cooling to −30 °C gave rise to a green crystalline material that was isolated by filtration and washed with cold pentane (3 × 1 mL) (50 mg, 70%). ^1H NMR (300 MHz, C_6D_6): δ 40.65 (overlaps), 34.78 (overlaps), 5.25 (overlaps), 3.13 (overlaps). Anal. Calcd: C, 65.50; H, 6.87. Found: C, 65.44; H, 6.79. μ_{eff} (Evans NMR method) = 2.0 μ_B.

Synthesis of (PNP)Rh(OC$_6$H$_4$F) (5). To a toluene solution (5 mL) of **2** (50 mg, 0.073 mmol) was added $NaOC_6H_4F$ (12 mg, 0.80 mmol) with vigorous stirring. After 16 h the volatile components were removed in vacuo, pentane was added, and the resultant green solution was filtered through Celite. Concentration and cooling to −30 °C gave rise to a green crystalline material that was isolated by filtration and washed with cold pentane (3 × 1 mL) (28 mg, 53%). ^1H NMR (300 MHz, C_6D_6): δ 43.47 36.45 (3H, br, overlapping), 17.79 (2H, br), 3.57 (24H, br), −16.39 (1H, br). ^{19}F NMR (282 MHz, C_6D_6): δ −105.17. Anal. Calcd: C, 59.82; H, 6.90. Found: C, 59.85; H, 6.95. μ_{eff} (Evans NMR method) = 2.0 μ_B.

Synthesis of (PNP)RhCl (6). *An alternative synthesis via hydrogen atom abstraction from* **8** *by TEMPO was reported elsewhere.*[43] To a solution of (PNP)Rh(OAc) (30 mg, 0.052 mmol) in benzene-d_6 (0.8 mL) was added Me_3SiCl (9.9 μL, 0.78 mmol). After 15 min the volatile components were removed in vacuo to give a green residue which could be recrystallized as a green crystalline solid from pentane. ^1H NMR (300 MHz, C_6D_6): δ 46.26 39.39 (2H, br, overlapping), 8.06 (overlaps with protio solvent), 3.51 (24H, br). Anal. Calcd: C, 55.08; H, 7.11. Found: C, 54.97; H, 7.03. μ_{eff} (Evans NMR method) = 1.9 μ_B.

Synthesis of (PNP)Rh(H)(OAc) (7). To a solution of **1** (180 mg, 0.29 mmol) in toluene (20 mL) was added an excess of acetic acid (50 μL, 0.88 mmol), and the mixture was heated to 85 °C for 16 h. Removal of the volatile components in vacuo gave rise to a red residue. The subsequent addition and removal of toluene and then pentane in vacuo gave a red powder (149 mg, 86%). ^1H NMR (300 MHz, C_6D_6): δ 7.55 (2H, dt, *J* = 8.6, *J* = 2.0, Ar*H*), 6.85 (2H, s, Ar*H*), 6.60 (2H, d, *J* = 8.0, Ar*H*), 2.41 (2H, m, C*H*), 2.19−2.05 (8H, m, C*H* and ArC*H*$_3$), 1.79 (3H, s, COC*H*$_3$), 1.30 (6H, dd, *J* = 15.8, *J* = 7.7, CHC*H*$_3$), 1.24−1.10 (12H, m, CHC*H*$_3$), 1.05 (6H, dd, *J* = 15.1, *J* = 7.4, CHC*H*$_3$), −23.77 (1H, dt, *J* = 30.5, *J* = 11.4, Rh*H*). $^{13}C\{^1H\}$ NMR (300 MHz, C_6D_6): δ 181.4 (s, CO), 162.3 (vt, *J* = 10.6, CN), 131.5 (s, C_{Ar}), 131.4 (s, C_{Ar}), 124.8 (s, C_{Ar}), 120.6 (vt, *J* = 3.0, C_{Ar}), 117.0 (vt, *J* = 5.6, C_{Ar}), 24.9 (vt, *J* = 12.3, PCH), 24.7 (vt, *J* = 11.6, PCH), 23.3 (s, $COCH_3$), 20.5 (s, $ArCH_3$), 18.7 (s, $CHCH_3$), 18.5 (s, $CHCH_3$), 18.3 (s, $CHCH_3$), 17.6 (s, $CHCH_3$). $^{31}P\{^1H\}$ NMR (300 MHz, C_6D_6): δ 52.3 (d, J_{RhP} = 107). Anal. Calcd: C, 56.85; H, 7.50. Found: C, 56.92; H, 7.41.

Synthesis of (PN(H)P)Rh(H)$_2$(OTf) (9). Exposure of a degassed solution of **2** (22.8 mg, 0.033 mmol) in benzene-d_6 (0.8 mL) in a 100 mL Teflon-stoppered flask to 1 bar of H_2 gave rise to a light yellow solution after 24 h. Transfer of the solution to a Young NMR tube gave the following data. ^1H NMR (300 MHz, C_6D_6): δ 9.51 (1H, s, N*H*), 7.12−7.05 (4H, m, Ar*H*), 6.75 (2H, d, *J* = 8.2, Ar*H*), 2.87−2.71 (2H, m, *H*), 2.13−1.96 (8H, m, C*H* + ArC*H*$_3$), 1.50 (6H, app quartet (dvt), *J* = 8, CHC*H*$_3$), 1.31 (6H, app quartet (dvt), *J* = 8, CHC*H*$_3$), 1.16 (6H, app quartet (dvt), *J* = 8, CHC*H*$_3$), 0.62 (6H, app quartet (dvt), *J* = 8, CHC*H*$_3$), −19.62 to −19.90 (2H, m, RhH_2). $^{13}C\{^1H\}$ NMR (75 MHz, CD_2Cl_2): δ 148.6 (vt, *J* = 8.8, CN), 137.3 (s, C_{Ar}), 135.1 (vt, *J* = 14.2, C_{Ar}), 134.8 (s, C_{Ar}), 131.4 (s, C_{Ar}), 125.0 (s, C_{Ar}), 27.8 (vt, *J* = 10.3, $CH(CH_3)_2$), 24.5 (vt, *J* = 11.4, $CH(CH_3)_2$), 21.1 (vt, *J* = 8.0, CH_3), 20.7 (s, CH_3), 20.0 (s, CH_3), 19.8 (s, CH_3), 18.9 (s, CH_3). ^{31}P NMR (121 MHz, C_6D_6): δ 65.1 (d, *J* = 114). ^{19}F NMR (282 MHz, C_6D_6): δ −77.9 (s). For complex **9**, a T_1 value of 541 ms was recorded at 298 K in toluene-d_8. As the sample was cooled, the single hydride signal broadened and split into two resonances (see the Supporting Information for a figure). At 210 K these were at −16.2 and −23.1 ppm with half-heights of 180 Hz.

Addition of H$_2$ to (PNP)Rh(OAc) (3). To a Young NMR tube containing a degassed solution of **3** (20 mg, 0.035 mmol) in C_6D_6 (0.6 mL) was added 1 bar of H_2. A color change from green to red was observed over a period of 15 min. Near-quantitative (95%) formation of (PNP)Rh(H)(OAc) (**7**) was noted by ^1H and ^{31}P NMR spectroscopy.

Addition of H$_2$ to (PNP)Rh(Cl) (6). To a Young NMR tube containing a degassed solution of **6** (16 mg, 0.032 mmol) in C_6D_6 (0.6 mL) was added 1 bar of H_2 and the solution was heated to 70 °C for 48 h. In addition to **6**, two other species were observed, including the previously characterized[37] (PNP)Rh(H)(Cl) (**8**). The third compound was assigned as (PN(H)P)Rh(H)$_2$(Cl) (**11**). Additional H_2 gas or further heating did not affect the ratio of these compounds. Select NMR data for **11** are as follows. ^1H NMR (300 MHz, C_6D_6): δ 8.31

(br, NH, overlapping with other resonances), −16.68 (1H, br, Rh−H), −18.33 (1H, br, Rh−H). ^{31}P NMR (121 MHz, C_6D_6): δ 67.2 (d, J_{RhP} = 114).

Addition of H_2 to (PNP)Rh(OC_6H_4F) (5). To a Young NMR tube containing a degassed solution of **5** (28 mg, 0.44 mmol) in C_6D_6 (0.6 mL) was added 1 bar of H_2 gas. After 16 h at 80 °C additional H_2 gas was added and the reaction mixture was heated for a further 16 h. Complete conversion to HOC_6H_4F and the previously reported[40] (PNP)Rh(H_2) (**10**) was observed by ^{1}H, ^{19}F, and ^{31}P NMR spectroscopy.

Observation of (PNP)Rh(HD) (10-*d*) and $T_{1,min}$ for (PNP)Rh(H_2) (10). To a C_6D_6 solution (1 mL) containing ca. 5 mg of (PNP)Rh(OTf) (**2**) was added an excess of CaH_2 (ca. 5 mg) followed by slow careful addition of D_2O (ca. 0.1 mL). After 24 h the solution was observed to be yellow and by ^{1}H and ^{31}P NMR spectroscopy a mixture of (PNP)Rh(H)(D) (major product) and (PNP)RhH_2 (minor product) was apparent. Collection of a ^{1}H{^{31}P} NMR spectrum allowed the J_{HD} coupling to be measured from the simplified splitting pattern. ^{1}H{^{31}P} NMR (500 MHz, C_6D_6): δ −13.76 (m, J_{RhH} = 20.0 Hz, J_{HD} = 18.3 Hz, Rh(*H*)(D)). For (PNP)RhH_2 (**10**) a $T_{1,min}$ value of approximately 39 ms was found at −48 °C (toluene-d_8).

X-ray Crystallography Details. In each case of **2**−**6**, multifaceted crystals of suitable size and quality were selected from representative samples of the same habit using an optical microscope and mounted onto a nylon loop. Low-temperature X-ray data were obtained on a Bruker APEXII CCD-based diffractometer (Mo sealed X-ray tube, λ(Mo Kα) = 0.71073 Å). All diffractometer manipulations, including data collection, integration, and scaling, were carried out using the Bruker APEXII software.[76] Absorption corrections were applied using SADABS.[77] Space groups were determined on the basis of systematic absences and intensity statistics, and structures were solved by direct methods and refined by full-matrix least squares on F^2. The structures were solved in the space groups noted in each case using XS[78] (incorporated in SHELXTL), and PLATON[79] was used to check for missed symmetry. Except where noted, all non-hydrogen atoms were refined with anisotropic thermal parameters.

Crystal structure data for **2**: $C_{27}H_{40}F_3NO_3P_2RhS$, 680.52 g/mol, monoclinic, space group $P2_1/c$; a = 17.845(5) Å, b = 10.692(3) Å, c = 18.267(6) Å, $\alpha = \gamma$ = 90°, β = 118.197(3)°, V = 3071.7(16) Å^3; Z = 4, ρ_{calcd} =1.472 g cm^{-3}; crystal dimensions 0.30 × 0.15 × 0.14 mm; diffractometer Bruker APEXII CCD; Mo Kα radiation, 110(2) K, $2\theta_{max}$ = 55.18°; 31780 reflections, 7092 independent (R_{int} = 0.0313), direct methods; absorption coefficient μ = 0.775 mm^{-1}, absorption correction multiscan (SADABS); refinement (against F_o^2) with SHELXTL V6.1, 417 parameters, 0 restraints, R1 = 0.0236 ($I > 2\sigma$) and wR2 = 0.0623 (all data), GOF = 1.036, residual electron density 0.478/−0.461 e Å^{-3}. The triflate moiety was found to be disordered over two positions with 65%:35% occupancy and was modeled and refined accordingly.

Crystal structure data for **3**: $C_{28}H_{43}NO_2P_2Rh$, 590.50 g/mol, orthorhombic, space group $P2_12_12_1$; a = 10.394(7) Å, b = 15.819(11) Å, c = 17.659(12) Å, $\alpha = \beta = \gamma$ = 90°, V = 2904(3) Å^3; Z = 4, ρ_{calcd} =1.351 g cm^{-3}; crystal dimensions 0.21 × 0.17 × 0.06 mm; diffractometer Bruker APEXII CCD; Mo Kα radiation, 163(2) K, $2\theta_{max}$ = 55.12°; 32228 reflections, 6663 independent (R_{int} = 0.0833), direct methods; absorption coefficient μ = 0.722 mm^{-1}), absorption correction multiscan (SADABS); refinement (against F_o^2) with SHELXTL V6.1, 318 parameters, 0 restraints, R1 = 0.0345 ($I > 2\sigma$) and wR2 = 0.0795 (all data), GOF = 1.025, residual electron density 0.408/−0.596 e Å^{-3}.

Crystal structure data for **4**: $C_{44}H_{55}NOP_2RhSi \cdot C_7H_8$, 898.96 g/mol, triclinic, space group $P\bar{1}$; a = 12.63(3) Å, b = 13.75(4) Å, c = 15.86(7) Å, α = 101.55(4)°, β = 96.30(5)°, γ = 115.73(3)°, V = 2370(14) Å^3; Z = 2, ρ_{calcd} = 1.260 g cm^{-3}; crystal dimensions 0.19 × 0.11 × 0.06 mm; diffractometer Bruker APEXII CCD; Mo Kα radiation, 150(2) K, $2\theta_{max}$ = 55.00°; 27126 reflections, 10767 independent (R_{int} = 0.0918), direct methods; absorption coefficient μ = 0.489 mm^{-1}, absorption correction multiscan (SADABS); refinement (against F_o^2) with SHELXTL V6.1, 525 parameters, 0 restraints, R1 = 0.0588 ($I > 2\sigma$) and wR2 = 0.1461 (all data), GOF = 0.916, residual electron density 0.913/−0.959 e Å^{-3}.

Crystal structure data for **5**: $C_{32}H_{44}FNOP_2Rh$, 642.55 g/mol, orthorhombic, space group $Pna2_1$; a = 26.147(15) Å, b = 14.062(8) Å, c = 8.548(5) Å, $\alpha = \beta = \gamma$ = 90°, V = 3143(3) Å^3; Z = 4, ρ_{calcd} =1.358 g cm^{-3}; crystal dimensions 0.18 × 0.09 × 0.08 mm; diffractometer Bruker APEXII CCD; Mo Kα radiation, 110(2) K, $2\theta_{max}$ = 54.96°; 32371 reflections, 7102 independent (R_{int} = 0.0616), direct methods; absorption coefficient μ = 0.676 mm^{-1}, absorption correction multiscan (SADABS); refinement (against F_o^2) with SHELXTL V6.1, 353 parameters, 1 restraints, R1 = 0.0332 ($I > 2\sigma$) and wR2 = 0.0693 (all data), GOF = 1.020, residual electron density 0.503/−0.417 e Å^{-3}.

Crystal structure data for **6**: $C_{26}H_{40}ClNP_2Rh$, 566.91 g/mol, monoclinic, space group $P2/c$; a = 11.506(4) Å, b = 9.706(4) Å, c = 18.323(5) Å, $\alpha = \gamma$ = 90°, β = 127.603(14)°, V = 1621.2(10) Å^3; Z = 2, ρ_{calcd} = 1.161 g cm^{-3}; crystal dimensions 0.20 × 0.12 × 0.09 mm; diffractometer Bruker APEXII CCD; Mo Kα radiation, 150(2) K, $2\theta_{max}$ = 55.56°; 18473 reflections, 3813 independent (R_{int} = 0.0700), direct methods; absorption coefficient μ = 0.719 mm^{-1}, absorption correction multiscan (SADABS); refinement (against F_o^2) with SHELXTL V6.1, 147 parameters, 0 restraints, R1 = 0.0316 ($I > 2\sigma$) and wR2 = 0.0805 (all data), GOF = 1.064, residual electron density 0.454/−0.415 e Å^{-3}. The "squeeze" protocol incorporated in PLATON was used to account for the disordered benzene solvent molecule found in the crystal lattice (verified by ^{1}H NMR) that could not be satisfactorily modeled.

■ ASSOCIATED CONTENT

Ⓢ Supporting Information

CIF files giving crystallographic data, DFT coordinate files, and a figure showing variable-temperature ^{1}H NMR spectra of **9**. This material is available free of charge via the Internet at http://pubs.acs.org.

■ AUTHOR INFORMATION

Corresponding Author

*E-mail for O.V.O.: ozerov@chem.tamu.edu.

Notes

The authors declare no competing financial interest.

■ ACKNOWLEDGMENTS

We are thankful for the support of this work by the U.S. National Science Foundation through the "Powering the Planet" Center for Chemical Innovation grant (CHE-0802907), the Welch Foundation (Grant A-1717), and the Dreyfus Foundation (Camille Dreyfus Teacher-Scholar Award to O.V.O.). J.R.W. expresses gratitude to the Nuclear Forensics Education Award Program for support. We thank Dr. Sylvain Gatard for a preliminary synthesis of compound **7** and Prof. Michael B. Hall for valuable discussions pertaining to the DFT studies.

■ REFERENCES

(1) (a) Takaoka, A.; Moret, M.-E.; Peters, J. C. *J. Am. Chem. Soc.* **2012**, *134*, 6695. (b) Takaoka, A.; Gerber, L. C. H.; Peters, J. C. *Angew. Chem., Int. Ed.* **2010**, *49*, 4088.
(2) Chan, Y. W.; Chan, K. S. *J. Am. Chem. Soc.* **2010**, *132*, 6920.
(3) Cui, X.; Xu, X.; Lu, H.; Zhu, S.; Wojtas, L.; Zhang, X. P. *J. Am. Chem. Soc.* **2011**, *133*, 3304.
(4) Pintauer, T.; Matyjaszewski, K. *Chem. Soc. Rev.* **2008**, *37*, 1087.
(5) de Bruin, B.; Budzelaar, P. H. M.; Gal, A. W. *Angew. Chem., Int. Ed.* **2004**, *43*, 4142.
(6) Mayer, J. M. *Acc. Chem. Res.* **2011**, *44*, 36.
(7) DeWitt, D. G. *Coord. Chem. Rev.* **1996**, *147*, 209.
(8) Pandey, K. K. *Coord. Chem. Rev.* **1992**, *121*, 1.

(9) Hansen, J.; Davies, H. M. L. *Coord. Chem. Rev.* **2008**, *252*, 545.

(10) Hay-Motherwell, R. S.; Koschmieder, S. U.; Wilkinson, G.; Hussain-Bates, B.; Hursthouse, M. B. *Dalton Trans.* **1991**, 2821.

(11) Masters, C.; Shaw, B. L. *J. Chem. Soc. A* **1971**, 3679.

(12) Takaoka, A.; Peters, J. C. *Inorg. Chem.* **2012**, *51*, 16.

(13) Mizutani, T.; Uesaka, T.; Ogoshi, H. *Organometallics* **1995**, *14*, 341.

(14) Cui, W.; Wayland, B. B. *J. Am. Chem. Soc.* **2004**, *126*, 8266.

(15) Li, S.; Cui, W.; Wayland, B. B. *Chem. Commun.* **2007**, 4024.

(16) Chan, K. S.; Li, X. Z.; Lee, S. Y. *Organometallics* **2010**, *29*, 2850.

(17) Sherry, A. E.; Wayland, B. B. *J. Am. Chem. Soc.* **1990**, *112*, 1259.

(18) Wayland, B. B.; Ba, S.; Sherry, A. E. *J. Am. Chem. Soc.* **1991**, *113*, 5305.

(19) Hetterscheid, D. G. H.; Klop, M.; Kichen, R. J. N. A. M.; Smits, J. M. M.; Reijerse, E. J.; de Bruin, B. *Chem. Eur. J.* **2007**, *13*, 3386.

(20) de Bruin, B.; Peters, T. P. J.; Thewissen, S.; Blok, A. N. J.; Wilting, J. B. M.; de Gelder, R.; Smits, J. M. M.; Gal, A. W. *Angew. Chem., Int. Ed.* **2002**, *41*, 2135.

(21) *The Chemistry of Pincer Compounds*; Morales-Morales, D., Jensen, C., Eds.; Elsevier: Amsterdam, 2007.

(22) Krumper, J. R.; Gerisch, M.; Suh, J. M.; Bergman, R. G.; Tilley, T. D. *J. Org. Chem.* **2003**, *68*, 9705.

(23) Gerisch, M.; Krumper, J. R.; Bergman, R. G.; Tilley, T. D. *J. Am. Chem. Soc.* **2001**, *123*, 5818.

(24) Feller, M.; Ben-Ari, E.; Gupta, T.; Shimon, L. J. W.; Leitus, G.; Diskin-Posner, Y.; Weiner, L.; Milstein, D. *Inorg. Chem.* **2007**, *46*, 10479.

(25) (a) Liang, L.-C.; Lin, J.-M.; Hung, C.-H. *Organometallics* **2003**, *22*, 3007. (b) Winter, A. M.; Eichele, K.; Mack, H.-G.; Potuznik, S.; Mayer, H. A.; Kaska, W. C. *J. Organomet. Chem.* **2003**, *682*, 149.

(26) Fan, L.; Foxman, B. M.; Ozerov, O. V. *Organometallics* **2004**, *23*, 326.

(27) For reviews on the chemistry of diarylamido-based PNP complexes, see: (a) Liang, L.-C. *Coord. Chem. Rev.* **2006**, *250*, 1152. (b) Ozerov, O. V. In *The Chemistry of Pincer Compounds*; Morales-Morales, D., Jensen, C., Eds.; Elsevier: Amsterdam, 2007; pp 287−309. (c) Mindiola, D. J.; Bailey, B. C.; Basuli, F. *Eur. J. Inorg. Chem.* **2006**, 3135.

(28) Fafard, C. M.; Adhikari, D.; Foxman, B. M.; Mindiola, D. J.; Ozerov, O. V. *J. Am. Chem. Soc.* **2007**, *129*, 10318.

(29) Gerber, L. C. H.; Watson, L. A.; Parkin, S.; Weng, W.; Foxman, B. M.; Ozerov, O. V. *Organometallics* **2007**, *26*, 4866.

(30) Fafard, C. M.; Chen, C.-H.; Foxman, B. M.; Ozerov, O. V. *Chem. Commun.* **2007**, 4465.

(31) Bacciu, D.; Chen, C.-H.; Surawatanawong, P.; Foxman, B. M.; Ozerov, O. V. *Inorg. Chem.* **2010**, *49*, 5328.

(32) Whited, M. T.; Grubbs, R. H. *Acc. Chem. Res.* **2009**, *42*, 1607.

(33) Cantat, T.; Graves, C. R.; Scott, B. L.; Kiplinger, J. L. *Angew. Chem., Int. Ed.* **2009**, *48*, 3681.

(34) Cavaliere, V. N.; Crestani, M. G.; Pinter, B.; Pink, M.; Chen, C.-H.; Baik, M.-H.; Mindiola, D. J. *J. Am. Chem. Soc.* **2011**, *133*, 10700.

(35) Melnick, J. G.; Radosevich, A. T.; Villagran, D.; Nocera, D. G. *Chem. Commun.* **2010**, *46*, 79.

(36) Calimano, E.; Tilley, T. D. *J. Am. Chem. Soc.* **2009**, *131*, 11161.

(37) Ozerov, O. V.; Guo, C.; Papkov, V. A.; Foxman, B. M. *J. Am. Chem. Soc.* **2004**, *126*, 4792.

(38) Weng, W.; Guo, C.; Moura, C. P.; Yang, L.; Foxman, B. M.; Ozerov, O. V. *Organometallics* **2005**, *24*, 3487.

(39) Gatard, S.; Çelenligil-Çetin, R.; Guo, C.; Foxman, B. M.; Ozerov, O. V. *J. Am. Chem. Soc.* **2006**, *128*, 2808.

(40) Weng, W.; Guo, C.; Çelenligil-Çetin, R.; Foxman, B. M.; Ozerov, O. V. *Chem. Commun.* **2006**, 197.

(41) Gatard, S.; Guo, C.; Foxman, B. M.; Ozerov, O. V. *Organometallics* **2007**, *26*, 6066.

(42) Gatard, S.; Chen, C.-H.; Foxman, B. M.; Ozerov, O. V. *Organometallics* **2008**, *27*, 6257.

(43) Smith, D. A.; Ozerov, O. V. *Chem. Commun.* **2011**, *47*, 10779.

(44) Surawatanawong, P.; Ozerov, O. V. *Organometallics* **2011**, *30*, 2972.

(45) Puri, M.; Gatard, S.; Smith, D. A.; Ozerov, O. V. *Organometallics* **2011**, *30*, 2472.

(46) Zhu, Y.; Smith, D. A.; Herbert, D. E.; Gatard, S.; Ozerov, O. V. *Chem. Commun.* **2012**, *48*, 218.

(47) Fout, A. R.; Basuli, F.; Fan, H.; Tomaszewski, J.; Huffman, J. C.; Baik, M.-H.; Mindiola, D. J. *Angew. Chem., Int. Ed.* **2006**, *45*, 3291.

(48) (a) Chan, K. S.; Leung, Y.-B. *Inorg. Chem.* **1994**, *33*, 3187. (b) Feng, M.; Chan, K. S. *Organometallics* **2002**, *21*, 2743. (c) Lee, S. Y.; Cheung, C. W.; Hsu, I.-J.; Chan, K. S. *Inorg. Chem.* **2010**, *49*, 9636.

(49) Bakac, A. *Dalton Trans.* **2006**, 1589.

(50) Zhang, X.-X.; Wayland, B. B. *J. Am. Chem. Soc.* **1994**, *116*, 7897.

(51) Mahoney, L. R.; Mendenhal, G. D.; Ingold, K. U. *J. Am. Chem. Soc.* **1973**, *95*, 8610.

(52) Kaim, W. *Inorg. Chem.* **2011**, *50*, 9752. van der Vlugt, J. I.; Reek, J. N. *Angew. Chem., Int. Ed.* **2009**, *48*, 8832.

(53) Adhikari, D.; Mossin, S.; Basuli, F.; Huffman, J. C.; Szilagyi, R. K.; Meyer, K.; Mindiola, D. J. *Inorg. Chem.* **2008**, *47*, 3676.

(54) Dunbar, K. R.; Haefner, S. C.; Pence, L. E. *J. Am. Chem. Soc.* **1989**, *111*, 5504.

(55) Dixon, F. M.; Farrell, J. R.; Doan, P. E.; Williamson, A.; Weinberger, D. A.; Mirkin, C. A.; Stern, C.; Incarvito, C. D.; Liable-Sands, L. M.; Zakharov, L. N.; Rheingold, A. L. *Organometallics* **2002**, *21*, 3091.

(56) Fan, L.; Yang, L.; Guo, C.; Foxman, B. M.; Ozerov, O. V. *Organometallics* **2004**, *23*, 4778. The FPNP ligand is only different by the F atoms in place of the Me groups para to the N atom.

(57) *POV-Ray−The Persistence of Vision Raytracer*, available at http://www.povray.org/.

(58) ORTEP plots were created using Ortep-3 for Windows: Farugia, L. *J. Appl. Crystallogr.* **1997**, *30*, 565.

(59) Wassenaar, J.; de Bruin, B.; Siegler, M. A.; Spek, A. L.; Reek, J. N. H.; van der Vlugt, J. I. *Chem. Commun.* **2010**, *46*, 1232.

(60) Gregor, L. C.; Chen, C.-H.; Fafard, C. M.; Fan, L.; Guo, C.; Foxman, B. M.; Gusev, D. G.; Ozerov, O. V. *Dalton Trans.* **2010**, *39*, 3195.

(61) Zhu, Y.; Chen, C.-H.; Fafard, C. M.; Foxman, B.; Ozerov, O. V. *Inorg. Chem.* **2011**, *50*, 7980.

(62) (a) Chaplin, A. B.; Weller, A. S. *Organometallics* **2011**, *30*, 4466. (b) Findlater, M.; Schultz, K. M.; Bernskoetter, W. H.; Cartwright-Sykes, A.; Heinekey, D. M.; Brookhart, M. *Inorg. Chem.* **2012**, *51*, 4672.

(63) (a) Kaska, W. C.; Nemeh, S.; Shirazi, A.; Potuznik, S. *Organometallics* **1988**, *7*, 13. (b) Xu, W.; Rosini, G. P.; Gupta, M.; Jensen, C. M.; Kaska, W. C.; Krogh-Jespersen, K.; Goldman, A. S. *J. Chem. Soc., Chem. Commun.* **1997**, 2273.

(64) (a) Gründemann, S.; Limbach, H. H.; Buntkowsky, G.; Sabo-Etienne, S.; Chaudret, B. *J. Chem. Phys. A* **1999**, *103*, 4752. (b) Gelabert, R.; Moreno, M.; Lluch, J. M.; Lledós, A.; Pons, V.; Heinekey, D. M. *J. Am. Chem. Soc.* **2004**, *126*, 8813.

(65) Kubas, G. J. *Proc. Natl. Acad. Sci. U.S.A.* **2007**, *104*, 6901.

(66) Fryzuk, M. D.; MacNeil, P. A.; Rettig, S. J. *J. Am. Chem. Soc.* **1987**, *109*, 2803.

(67) Osborn, J. A.; Jardine, F. H.; Young, J. F.; Wilkinson, G. *J. Chem. Soc. A* **1966**, 1711.

(68) Heaton, B. T.; Iggo, J. A.; Jacob, C.; Nadarajah, J.; Fontaine, M. A.; Messere, R.; Noels, A. F. *Dalton Trans.* **1994**, 2875.

(69) Stephens, P. J.; Devlin, F. J.; Chabalowski, C. F.; Frisch, M. J. *J. Phys. Chem.* **1994**, *98*, 11623−11627.

(70) Becke, A. D. *J. Chem. Phys.* **1993**, *98*, 5648−5652.

(71) Lee, C.; Yang, W.; Parr, R. G. *Phys. Rev. B* **1988**, *37*, 785−789.

(72) Frisch, M. J.; Trucks, G. W.; Schlegel, H. B.; Scuseria, G. E.; Robb, M. A.; Cheeseman, J. R.; Scalmani, G.; Barone, V.; Mennucci, B.; Petersson, G. A.; Nakatsuji, H.; Caricato, M.; Li, X.; Hratchian, H. P.; Izmaylov, A. F.; Bloino, J.; Zheng, G.; Sonnenberg, J. L.; Hada, M.; Ehara, M.; Toyota, K.; Fukuda, R.; Hasegawa, J.; Ishida, M.; Nakajima, T.; Honda, Y.; Kitao, O.; Nakai, H.; Vreven, T.; Montgomery, J. A., Jr.; Peralta, J. E.; Ogliaro, F.; Bearpark, M.; Heyd, J. J.; Brothers, E.; Kudin, K. N.; Staroverov, V. N.; Kobayashi, R.; Normand, J.; Raghavachari, K.; Rendell, A.; Burant, J. C.; Iyengar, S. S.; Tomasi, J.; Cossi, M.; Rega,

N.; Millam, J. M.; Klene, M.; Knox, J. E.; Cross, J. B.; Bakken, V.; Adamo, C.; Jaramillo, J.; Gomperts, R.; Stratmann, R. E.; Yazyev, O.; Austin, A. J.; Cammi, R.; Pomelli, C.; Ochterski, J. W.; Martin, R. L.; Morokuma, K.; Zakrzewski, V. G.; Voth, G. A.; Salvador, P.; Dannenberg, J. J.; Dapprich, S.; Daniels, A. D.; Farkas, O.; Foresman, J. B.; Ortiz, J. V.; Cioslowski, J.; , and Fox, D. J. *Gaussian 09, Revision B.01*; Gaussian, Inc., Wallingford, CT, 2009.

(73) (a) Hehre, W. J.; Ditchfield, R.; Pople, J. A. *J. Chem. Phys.* **1972**, *56*, 2257−2261. (b) McLean, A. D.; Chandler, G. S. *J. Chem. Phys.* **1980**, *72*, 5639−5648. (c) Frisch, M. J.; Pople, J. A.; Binkley, J. S. *J. Chem. Phys.* **1984**, *80*, 3265−3269.

(74) 6-31(d′) differs from 6-31(d) and 6-31G* by the addition of a single diffuse function which is optimized specifically for each of the second-row (B−F) elements.

(75) Kuechle, W.; Dolg, M.; Stoll, H.; Preuss, H. *J. Chem. Phys.* **1994**, *100*, 7535−7542.

(76) *APEX2, Version 2 User Manual, M86-E01078*; Bruker Analytical X-Ray Systems: Madison, WI, 2006.

(77) Sheldrick, G. M. *SADABS, Program for Absorption Correction for Data from Area Detector Frames*; University of Göttingen, Göttingen, Germany, 2008.

(78) Sheldrick, G. M. *Acta Crystallogr., Sect. A: Found. Crystallogr.* **2008**, *A64*, 112.

(79) Spek, A. L. *PLATON, A Multipurpose Crystallographic Tool*; Utrecht University, Utrecht, The Netherlands, 1998.